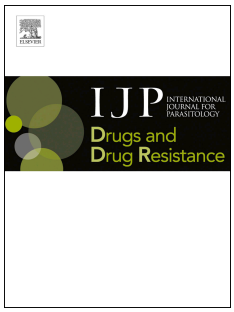

Metabolomics study of 3-O-*p*-(*Z/E*)-coumaroyltormentic acid-treated *Trypanosoma brucei brucei*

Lúcia Mamede, Fanta Fall, Madeline Vast, Kristelle Hughes, Giorgia Martelli, Francesco Caligiore, Bernadette Govaerts, Paul A.M. Michels, Michel Frédérich, Joëlle Quetin-Leclercq

PII: S2211-3207(25)00018-1

DOI: https://doi.org/10.1016/j.ijpddr.2025.100595

Reference: IJPDDR 100595

To appear in: *International Journal for Parasitology: Drugs and Drug Resistance*

Received Date: 1 December 2024

Revised Date: 27 March 2025

Accepted Date: 15 April 2025

Please cite this article as: Mamede, L., Fall, F., Vast, M., Hughes, K., Martelli, G., Caligiore, F., Govaerts, B., Michels, P.A.M., Frédérich, M., Quetin-Leclercq, J., Metabolomics study of 3-O-*p*-(*Z/E*)-coumaroyltormentic acid-treated *Trypanosoma brucei brucei*, *International Journal for Parasitology: Drugs and Drug Resistance*, https://doi.org/10.1016/j.ijpddr.2025.100595.

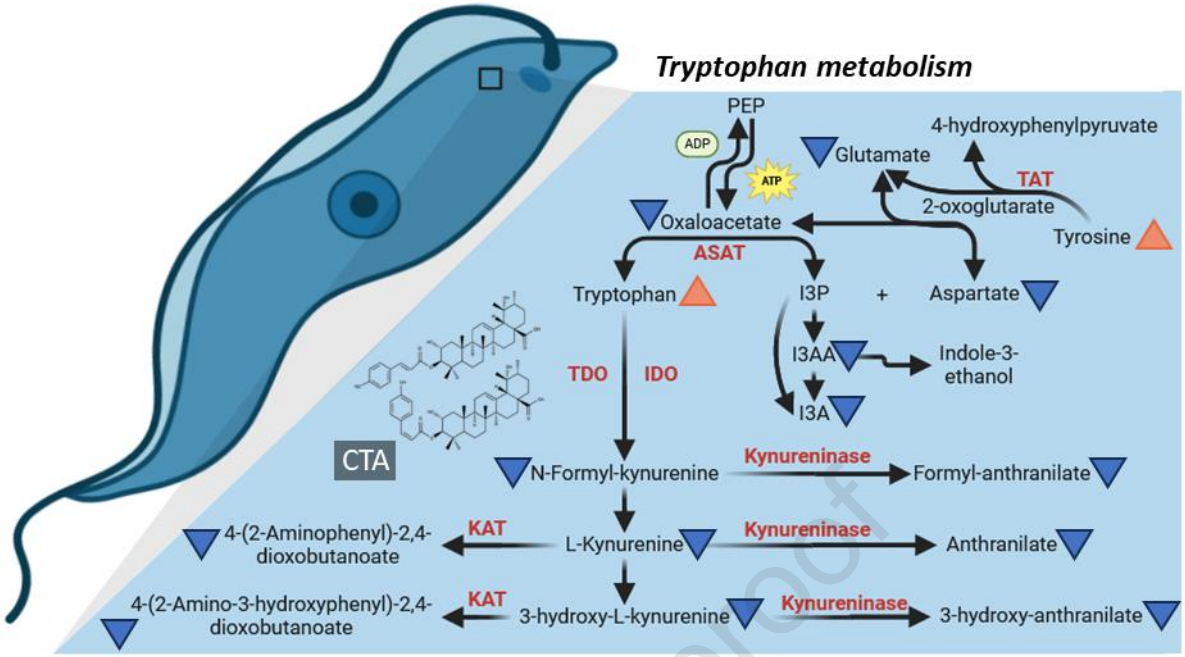

Metabolomics study of 3-O-*p*-(*Z/E*)-coumaroyltormentic acid-treated *Trypanosoma brucei brucei*

Lúcia Mamede[1,2*], Fanta Fall[1], Madeline Vast[3], Kristelle Hughes[1], Giorgia Martelli[1], Francesco Caligiore[4], Bernadette Govaerts[3], Paul A.M. Michels[5], Michel Frédérich[2], Joëlle Quetin-Leclercq[1]

[1]Pharmacognosy Research Group, Louvain Drug Research Institute (LDRI), UCLouvain, Brussels, Belgium.

[2]Laboratory of Pharmacognosy, Center of Interdisciplinary Research on Medicines (CIRM), University of Liège, Belgium.

[3]Institute of Statistics, Biostatistics and Actuarial Sciences (ISBA/LIDAM), Université catholique de Louvain (UCLouvain), Louvain-la-Neuve, Belgium.

[4] de Duve Institute and WELBIO, UCLouvain, Avenue Hippocrate 75, 1200, Brussels, Belgium.

[5]School of Biological Sciences, The University of Edinburgh, Scotland

*Corresponding author

ABSTRACT

Trypanosomiasis is a parasitic disease for which new treatments are needed due to the frequent occurrence of adverse side effects of current available drugs. Natural compounds found in traditionally used plants offer opportunities to discover innovative compounds that could prove pivotal to antitrypanosomal drug development. 3-O-*p*-(*Z/E*)-coumaroyltormentic acids (CTA) were isolated first from the West Africa-native tree *Vitellaria paradoxa* and have demonstrated quite selective *in vitro* and *in vivo* antitrypanosomal activity, despite the unknown mode of action. In this study, a metabolomics analysis using the data from both LC-HR-MS and ^{1}H-NMR described CTA's effects on *Trypanosoma brucei* after 3 h exposure under 5 or 10 x EC_{50}. Our study shows CTA's activity impacted tryptophan metabolism and reveals potential targets in different branches of this metabolism. Our results demonstrate a likely presence of enzymes dedicated to tryptophan, like a tryptophan aminotransferase, tryptophan 2,3-dioxygenase and/or indoleamine 2,3-dioxygenase, and other enzymes of the kynurenine pathway, despite the absence of their description thus far in this species. These data further implicate that CTA's toxic effect on the tryptophan metabolism may be attributed to the decrease of the intracellular level of essential aspartate, resulting from inhibition of its aminotransferase. In resume, our study shines light on the likelihood of the tryptophan metabolism pathway presenting innovative targets toward the development of antitrypanosomal drugs. These require confirmation through functional and enzymatic studies.

KEYWORDS: Metabolomics, 3-O-p-E/Z-coumaroyltormentic acids, *Trypanosoma brucei brucei*, Mass Spectrometry, Nuclear Magnetic Resonance

INTRODUCTION

Trypanosoma brucei is the parasite responsible for African sleeping sickness, a vector-borne disease that accounts for approximately 1,000 reported cases annually (Barrett et al. 2024; "WHO | Human African trypanosomiasis" n.d.). Depending on the stage of the disease and the parasite species (*T. b. gambiense* or *T. b. rhodesiense*), six treatments are recommended by the World Health Organization (WHO) (Fall et al. 2022; "WHO | Human African trypanosomiasis" n.d.). Pentamidine and suramin are recommended for specific stages of *T. b. gambiense* and *T. b. rhodesiense* infections, respectively (Kasozi et al. 2022; Wiedemar et al. 2020). Melarsoprol is used in case of *T. b. rhodesiense* infection, while other treatments such as administration of eflornithine, the nifurtimox-eflornithine combination (NECT), and fexinidazole are recommended in *T. b. gambiense* trypanosomiasis (Kasozi et al. 2022). However, most of these treatments are associated with significant side effects, *e.g.* hypoglycemia, hypotension, nephrotoxicity, reactive encephalopathy, prompting research into alternative options. Nature offers such alternatives, with traditionally used plants known to be the source of many possibilities for the discovery of innovative active compounds with lower toxicity profiles (Fall et al. 2022; Franco et al. 2018; Hannaert 2011).

In an effort to discover new lead compounds, Catteau et al. isolated a mixture of 3-O-*p*-(*Z/E*)-coumaroyltormentic acids from the West Africa-native tree *Vitellaria paradoxa* (Catteau et al. 2021), which demonstrated promising antitrypanosomal activity. As the two forms (*E* and *Z*) naturally transform into each other and occurred mixed with the corresponding ferulic esters, which have a similar structure and also transform into each other, the mixture was used for testing and called CTA. The EC_{50} and selectivity index (SI) values (EC_{50} *Trypanosoma brucei brucei* (*T. b. brucei*) = 0.5 ± 0.4 mg/L or 0.7 ± 0.6 µM; SI = 43.8 compared to human non-cancerous fibroblasts – WI38 cells) of 3-O-*p*-(*Z/E*)-coumaroyltormentic acids adhered to the criteria proposed by Pink et al. for selecting antiparasitic hit compounds: $EC_{50} \leq 1$ mg/L and SI > 20 (Catteau et al. 2021; Pink et al. 2005). Consequently, the mixture underwent *in vivo* testing for acute toxicity and antitrypanosomal activity. The results indicated an absence of acute toxic symptoms at a cumulative dose of 100 mg/kg and demonstrated reduced parasitemia (on day 4 post-infection) and enhanced survival of infected mice when administered at a dose of 50 mg/kg/day via intraperitoneal

injection (Catteau et al. 2021). These compounds were also isolated from an *in vitro*-cultivated apple cell extract with higher yields to obtain a more accessible production (Leclercq et al. 2020).

Despite this promising activity, CTA's mode of action remains unclear and could prove important to develop new therapeutic hits. Metabolomics is an excellent tool for conducting the analysis of the global metabolism of the parasite after exposure to a compound of interest to identify the metabolites (MW < 1500 Da) that indicate how the parasite is being affected. To elucidate the antitrypanosomal mode of action of CTA, metabolomics analysis employing hydrophilic interaction liquid chromatography (HILIC) coupled with high-resolution mass spectrometry (HRMS), mainly allowing the analysis of polar metabolites in the *T. b. brucei* metabolome, which are the most abundant (Fall et al. 2022; Johnston et al. 2019), and proton Nuclear Magnetic Resonance (^{1}H-NMR) spectroscopy were conducted. The combination of these two analytical methods allows for the coverage of a wide range of molecules with diverse physicochemical properties that could otherwise be missing in the final picture. Extraction was performed using a method showing the best quantitative criteria including the number, intensity, reproducibility, and variability of features, as well as qualitative criteria such as the specific coverage of relevant metabolites (Fall et al. 2024). Our study found significant changes related to tryptophan metabolism due to CTA treatment, giving grounds to a debate on whether this pathway could be explored for the development of antitrypanosomal drugs.

MATERIALS AND METHODS

1. Reagents

LC-MS-grade ammonium formate, formic acid (98%), and fetal bovine serum (FBS) were procured from Sigma (Bornem, Belgium). HMI-9 medium, DMSO and phosphate-buffered saline (PBS) were obtained from Thermo Fisher Scientific (Merelbeke, Belgium). Alamar Blue was obtained from Bio-Rad (Temse, Belgium). Absolute ethanol, methanol, acetonitrile and LC-MS-grade water were obtained from VWR (Louvain, Belgium). Trimethylsilyl-3-propionide acid-d4 (TMSP) and deuterium oxide (D_2O, 99.96% D) were obtained from CortecNet (France). Phosphate buffer powder was supplied by Sigma–Aldrich (Karlsruhe, Germany).

2. Extraction of apple cell culture and purification of CTA

The "Cox's Orange Pippin" callus-derived apple cell powder (*Malus domestica*) was provided by the Luxembourg Institute of Science and Technology (LIST). A quantity of 48.75 g of the apple cell powder was mixed with 7.5 L of ethanol (EtOH) and subjected to a 10-min sonication, followed by agitation for 4 h at 4 °C. The sample was filtered (150 mm Dia, Whatman®) using a vacuum pump (LABOPORT®) and evaporated under reduced pressure to a dry extract using a rotary evaporator (Büchi Labortechnik). The dry extract obtained (~13.65 g) was dissolved in EtOH and coated onto 41 g of silica C18 (Lichroprep® RP18 40-63 µm, Merck Millipore) according to a method previously described (Leclercq et al. 2020). Then, the sample was fractionated using thirteen 5 g C18 Isolute® Solide-Phase extraction (SPE) cartridges (Biotage), previously conditioned. The conditioning was performed with 10 mL of EtOH, followed by 10 mL of 1:1 EtOH/H_2O (v/v) and finally 10 mL of 25:75 EtOH/H_2O (v/v). After conditioning, approximately 4 g of the sample coated in C18 silica were added to each cartridge and eluted under vacuum with 2x10 mL each of 25:75 EtOH/H_20 (v/v), resulting in fractions F1 and F2, 1:1 EtOH/H_2O (v/v) (F3-F4), 65:35 EtOH/H_2O (v/v) (F5-F6), 75:25 EtOH/H_2O (v/v) (F7-F8), 85:15 EtOH/H_2O (v/v) (F9-F10) and 100:0 EtOH/H_2O (v/v) (F11-F12). Each fraction was evaporated under reduced pressure with a rotary evaporator. Fractions F1 to F12 and a reference of CTA, obtained previously in the lab, were analysed using an Accela HPLC (Thermo Fisher Scientific). For each fraction, a solution at a concentration of 10 mg/mL was prepared in methanol, filtered (0.45 µm PTFE Membrane, Whatman®) and 20 µL were injected in the analytical HPLC. The column used was a Luna C18, 250x4.6 mm packed with 5 µm particles (Phenomenex). The binary solvent system was: solvent A, water and solvent B, acetonitrile/methanol 40:35 (v/v). The gradient elution program was as follows: 0-6 min 80% B; 6-13 min 80%-77% B; 13-13:20 min 77%-80% B; 13:20-30 min 80% B and the flow rate was set to 0.80 mL/min. Peaks were detected at 210 nm and 235 nm. Fractions presenting the same chromatographic profile and containing the reference peak were pooled to a single fraction: Ft.

The pooled fraction Ft was purified by preparative HPLC using a Luna C18, 250x30 mm (5 µm particles, Phenomenex) column. The flow rate was set at 34 mL/min, using the same method as developed for analytical HPLC. Nine purified fractions were collected. Direct infusion-HR-MS was performed on a 10 mg/mL solution of the purified fraction containing CTA in negative electrospray ionization mode using an LTQ XL Orbitrap mass spectrometer of the MASSMET platform (Thermo Fisher Scientific). Mass spectra data were recorded in full scan MS between 100

and 1000 *m/z*. The ESI inlet settings were: flow rate, 100 µL/min, capillary temperature and voltage at 275 °C and -23 V, respectively. The sheath and auxiliary (N_2) gas flow rates were set at 15 a.u. The purification of 3-*O*-*p*-(*Z/E*)-coumaroyltormentic acids from the apple cell powder was confirmed by HPLC and HRMS data showing that they correspond to the main peak, and that a small peak (about 30%) corresponding to 3-*O*-*p*-(*Z/E*)-feruloyltormentic acids was also present (Supplementary data Figure 1). This mixture was named CTA and used for the metabolomic study.

3. Parasite culture and sample preparation

Parasites used were bloodstream forms (BSF) of the subspecies *T. brucei brucei* strain Lister 427 (Molteno Institute in Cambridge, UK), the cell line described previously (Biebinger et al. 1997). *T. brucei* BSF were cultured *in vitro* at 37 °C with 5% CO_2 in HMI-9 medium containing 10% (v/v) heat-inactivated fetal bovine serum (FCS), $NaHCO_3$ (36 mM), hypoxanthine (1 mM), sodium pyruvate (1 mM), thymidine (0.16 mM), bathocuprone (0.04 mM), β-mercaptoethanol (20 mM) and L-cysteine (150 mM) (Hirumi and Hirumi 1994). Parasites were maintained at densities between 1 x 10^6/mL and 1.5 x 10^6/mL and 100- or 1000-fold dilution was done every 2 or 3 days. The count of viable trypanosomes, assessed based on their motility, was determined using a Bürker chamber. The EC_{50} value (0.16 µg/mL) of CTA was determined in a 72 h Alamar Blue assay and should be read as the effective concentration resulting in 50% reduction of the redox state of the *in vitro* cultured cells that is taken as a measure of the inhibition of cell proliferation. Three conditions: control, CTA at 5 x EC_{50} and 10 x EC_{50} were tested and collected after 3 h of incubation for metabolomics extraction and analysis. Cultures were done in triplicate *i.e.* 18 flasks in total. Parasites were transferred to microcentrifuge tubes and rapidly quenched in a dry ice/ethanol mixture for 20 s. Following this, samples were subjected to centrifugation at 1250 relative centrifugal force (rcf) for 10 min. A liquid-liquid extraction was carried out using a 1.5 mL mixture of acetonitrile, methanol, and water (4/4/2 v/v/v). The samples were vigorously vortexed and incubated for 20 min at 20 °C, after which they were dried under vacuum conditions before being reconstituted in 150 µL of ultrapure water. Subsequently, the reconstituted samples were centrifuged at 4000 rcf for 2 min, and the resulting supernatant was transferred into an LC-HRMS vial. In addition to the samples, quality controls (QC) were prepared by pooling 10 µL from each sample and subjecting them to multiple injections. Alternatively, for NMR analysis, the dried samples were dissolved in 400 µL of buffered D_2O at pH 7.4, with TMSP used as an internal

reference. These prepared samples were then transferred to 3 mm NMR tubes (Bruker) for analysis. Additional timepoints were studied, including a preliminary 5h, 14h, 24h and 48h experiment at EC_{50} and 2x EC_{50}, and a second study featuring only 3h and 5h at 5 and 10x EC_{50}, in the same conditions. Shorter time pulses were associated with better separation between treated and untreated parasites. Results from 5h did not yield concrete results, potentially due to general cellular death pathways being already activated. Thus, a shorter time pulse was pursued in subsequent studies to zoom in on CTA's effect on the trypanosome.

4. Instrumentation, data acquisition and processing

LC-HR-MS analyses were performed using a SeQuant® ZIC®-pHILIC 5 µm polymer column (150 x 4.6 mm; Supelco) at a constant flow rate of 0.3 mL/min with an Agilent 1290 HPLC system coupled to an Agilent 6546 LC/Q-TOF mass spectrometer. 10 µL of sample were analyzed in electrospray ionization (ESI) positive and negative modes. For the positive mode, mobile phase A consisted of 10 mM ammonium formate with 0.1% formic acid and phase B of 100% acetonitrile. The mobile phase profile consisted of the following steps and linear gradients: 0 – 3 min at 95% B; 3 – 25 min from 95 to 5% B; 25 – 30 min 5% B; 30 – 31 min from 5 to 95% B; 31 – 40 min 95% B. An *m/z* range from 50 to 1000 was acquired with a frequency of 1 per second by adding 9287 transients, and the source was operated with the following settings: ESI spray voltage 3500 V, sheath gas 325 °C at 10 L/min, nebulizer pressure 40 psig and drying gas 225 °C at 8 L/min. For the negative mode, mobile phase A consisted of 20 mM ammonium carbonate pH 9.2 and phase B of 100% acetonitrile. The mobile phase profile consisted of the following steps and linear gradients: 0 – 3 min at 92% B; 3 – 25 min from 92 to 8% B; 25 – 30 min from 8 to 8 % B; 30 – 31 min from 8 to 92% B; 31 – 40 min from 92 to 92% B. An *m/z* range from 60 to 1050 was acquired with a frequency of 1 per second by adding 9284 transients with the following ESI settings: ESI spray voltage 3500 V, sheath gas 275 °C at 12 L/min, nebulizer pressure 35 psig and drying gas 225 °C at 13 L/min.

The raw files were converted to mzXML format using ProteoWizard software (Adusumilli and Mallick 2017) and centwave was utilized for peak picking detection. The data were preprocessed with Workflow4Metabolomics under Galaxy (Giacomoni et al. 2015). To enhance the quality of the metabolomics analysis the procedures encompassed the removal of background noise and the preservation of robust features within the dataset. To ensure data consistency, samples were

subjected to normalization against a quality control (pooled sample) reference. Subsequently, features in the spectral data of biological samples were selectively retained if their intensities exceeded a two-fold threshold in comparison to blank samples; otherwise, they were excluded from further analysis. A Log_{10} transformation was applied to the samples, followed by Pareto normalization, aiming to achieve a Gaussian distribution of the dataset.

^{1}H-NMR spectra were obtained utilizing a Bruker NEO Ultrashield Plus 700 MHz instrument equipped with a helium cryoprobe. ^{1}H-NMR experiments were executed employing a CPMG sequence, consisting of 128 scans, within a spectral width of 20 ppm. All spectra underwent manual phasing and baseline correction using TopSpin v4. Spectra were stacked and aligned across the δ0.5-9.5 ppm range using MestReNova v14. The spectra were further normalized to the sum of intensities and segmented into 0.04 ppm buckets to originate a bucket table. Spectral annotations were accomplished by referencing the Chenomx NMR Suite 9.0 database.

5. Statistical analysis and functional analysis

Univariate analyses, such as ANOVA, and multivariate analyses, including PCA and PLS-DA were employed to visualize the changes induced by the treatment effect on the *T. b. brucei*. The p-values from the ANOVA were corrected for multiple testing using the FDR correction method. These analyses were carried out using MetaboAnalyst v. 5.0. Identification of impacted pathways was conducted using the Mummichog algorithm, as proposed by Li et al. (Li et al. 2013) and implemented in MetaboAnalyst v. 6.0 without additional corrections. The KEGG pathway library for *T. b. brucei* was used as pathway library for this analysis. Since MetaboAnalyst outputs contain the identifiers of the metabolites but not their names, the package KEGGREST was used in R to retrieve the name of the metabolites in the significant pathways as found by the Mummichog algorithm and crossed with the KEGG pathway library.

RESULTS

Biological studies often require large amounts of purified compounds, which can become an issue when the source species are protected or threatened. As such, a patent was obtained on the production of enriched triterpenic derivatives extracts from apple cells in culture and purification of CTA that then can be used for further testing (Leclercq et al. 2020). Using this methodology, CTA was purified and tested in the metabolomics study.

Untargeted metabolomics through LC-HR-MS and ^{1}H-NMR reveals CTA's candidate targets responsible for antitrypanosomal effect

The metabolomics analysis was performed through an untargeted approach of BSF *T. b. brucei* treated with CTA for 3 h under different conditions (control, treated at 5 x EC_{50}, and treated at 10 x EC_{50}). The parasite's metabolome was analyzed using both HR-MS and ^{1}H-NMR to reveal the metabolites potentially involved in CTA's established antitrypanosomal activity.

HR-MS-negative and HR-MS-positive analyses detected 9595 and 6113 features, respectively, which, after applying robustness filters to eliminate false peaks and background noise, accounted for 7923 in negative mode and 3944 features in positive mode. Meanwhile, ^{1}H-NMR spectra were converted into a bin table constituted by 197 bins per sample which were mean centered before statistical analysis.

All metabolites obtained from HR-MS and ^{1}H-NMR were subjected to multivariate statistical analyses such as PCA to visualize the separation between the different groups (Figure 1.1). In both HR-MS-negative and ^{1}H-NMR analyses, clear separation among the three groups was observed as explained by the principal components. The cumulative contribution of the first two principal components (PC1+PC2) accounted for a significant proportion of the total variance observed in these two analytical conditions, amounting to 74.8% and 92.6%, respectively. However, this separation is less pronounced in the HR-MS-positive analysis.

Partial Least-Squares Discriminant Analysis (PLS-DA) was also performed on our data and the scores plot is shown in Figure 1.2. The PLS-DA model revealed a more pronounced separation among the three sample groups across all analytical conditions: HR-MS-negative, HR-MS-positive, and ^{1}H-NMR. The cumulative contribution of the first two principal components (PC1+PC2) accounted for 68.3%, 80.6%, and 86.9% of the total variance, respectively. Model prediction capabilities showed the data were well-fitted for HR-MS-negative and ^{1}H-NMR, with Q^2 above 0.78 and R^2 values exceeded 0.9, indicating that the variance was adequately explained by the latent model components (Supplementary Data Figure 2). However, this was not the case for HR-MS-positive, where R^2 was less than 0.3 and Q^2 was negative for the first component, revealing overfitting data (Chong et al. 2019; Féraud et al. 2017; Karaman et al. 2015).

Despite the potential for the data analysis provided by the separation and goodness of fit in the PLS-DA model, the extent of the data (not annotated at this point) made biological interpretation harder to achieve. As such, other statistical models were pursued in order to facilitate both annotation and functional interpretation.

Initial analysis focused on the results of ANOVA to comprehensively examine the significant features when comparing the three sample groups in detail. Importantly, the HR-MS-positive data only elicited two significant features with a level 4 identification (*m/z*= 453.1675 RT=466.3 s; *m/z*= 254.1081 RT=1038.1 s). Considering the lack of group separation and significant features, positive ionization data were not further analyzed. In the case of HR-MS-negative data, a total of 2540 features exhibited significance ($p<0.05$). Lastly, during the statistical analyses conducted for ^{1}H-NMR data, 59 bins were identified as statistically significant.

HR-MS-negative data were further analyzed with an algorithm available in MetaboAnalyst v. 6.0 which combines the metabolite identification based on HRMS data and pathway enrichment analysis to achieve the identification of pathways that are statistically significantly impacted by the treatment without prior identification of the metabolites. The EASE score was used to identify the significant pathways. EASE is a score built upon removing a significant compound from a pathway and recalculating the Fisher's exact test p-value to confirm significance. Table 1 displays the only significant metabolic pathway with the significant metabolites identified by HR-MS-negative after applying the EASE score (EASE <0.05) (the full Pathway Enrichment table can be found in Supplementary Data Table 1).

ANOVA analysis of the features detected by HR-MS-negative ionization reveal a smaller ANOVA identified match, which decreases further after potential annotation as seen in Supplementary Data Figure 3. Despite a significant number of features detected, a big discrepancy is found between the total amount of detected features and those that were confidently annotated (whether significant or not). Finally, 30 significant features that potentially correspond to metabolites belonging to the significant pathway identified by functional analysis were associated with CTA treatment. HR-MS detection often has matrix effects and multiple ions from the same metabolite may also be observed, explaining why the number of ANOVA significant features is much lower than the number of detected features, which may, especially after correction and filters performed during data analysis, not represent a loss of data, but rather a refining. More importantly, an untargeted analysis aims to

capture as much of the metabolome as possible, which naturally translates into a higher necessity of filtering to discern which metabolites are relevant for a certain effect.

Table 1. Significant pathway identified by functional analysis of the HR-MS data in negative mode with the EASE score, significant potential compounds and their query mass, retention time and compound form. Fold-change comparing control to 10 x EC_{50}.

Pathway	EASE score	Significant potential compounds	Query Mass *(m/z)*	Retention time (s)	Fold change (*p*-value ANOVA)	Compounds form	Level of identification according to the metabolomic standard initiative (Sumner et al. 2007)
Tryptophan metabolism	0.024483	Anthranilate	136.0404	1157.9	-2.7 (0.000220)	$[M-H]^-$	1
		3-Hydroxyanthranilate	152.0354539	291.2	-2.1 (0.032663)	$[M-H]^-$	2
		2-Oxoadipate	159.0298	1173.0	-3 (0.001466)	$[M-H]^-$	2
		Indole-3-acetaldehyde	179.0350086	1120.9	-2.4 (0.000522)	$[M+Na-2H]^-$	2
		Formylanthranilate	224.0564	186.6	-2.8 (0.011455)	$[M+CH_3COO]^-$	2
		4-(2-Aminophenyl)-2,4-dioxobutanoate	206.0457964	1184.8	-2.5 (0.000176)	$[M-H]^-$	2
		5-Hydroxyindoleacetate	236.0564	641.5	-2.7 (0.010746)	$[M+HCOO]^-$	2
		4-(2-Amino-3-hydroxyphenyl)-2,4-dioxobutanoate	263.0648779	703.2	-2.2 (0.0222)	$[M+ACN-H]^-$	2
		L-Kynurenine	267.09853	1154.2	-2.5 (0.000141)	$[M+CH_3COO]^-$	2
		3-Hydroxy-L-kynurenine	269.0779	976.1	-2.6 (0.015205)	$[M+HCOO]^-$	2
		L-Formylkynurenine	276.0981711	964.8	-2.8 (0.00125)	$[M+ACN-H]^-$	2
		(S)-3-Hydroxybutanoyl-CoA	873.1246449	508.4	-2.9 (0.000103)	$[M+Na-2H]^-$	2

The EASE score strongly suggests that tryptophan metabolism is affected by CTA. All 12 metabolites listed in Table 1 can be formed from this amino acid according to standard metabolic schemes. A heatmap was generated to visually correlate the effects caused by CTA on the significant compounds in Table 1 (Figure 2A). For each of these metabolites there is a lower fold change related to 10 x EC_{50} treatment with CTA in comparison with other groups. These metabolites represent two branches of tryptophan metabolism (Figure 2B). The overall direction in which the metabolites across the two branches change suggests an inhibition early in tryptophan metabolism, which could have occurred at the import of this amino acid into the trypanosome or immediately after it in each of the branches. However, the NMR data indicated a significant increase in the intracellular level of tryptophan (see below), rendering transport inhibition unlikely.

One branch of tryptophan metabolism involves the so-called kynurenine pathway (KP). Considering the negative fold change of its first intermediate, N-formylkynurenine, in comparison with the control group, it is possible that the enzyme catalyzing its production from tryptophan is a CTA target (Figure 2B). The formation of N-formylkynurenine is usually catalyzed in cells by tryptophan 2,3-dioxygenase (TDO, EC 1.13.11.11) and/or indoleamine 2,3-dioxygenase (IDO, EC 1.13.11.52), but neither of these enzymes or genes potentially coding for them have so far been identified in *Trypanosoma* species (Ball et al. 2014). If an enzyme metabolizing N-formylkynurenine was affected, an accumulation of this metabolite could be expected, which doesn't seem to be the case. On the contrary, levels of two metabolites formed from it (L-kynurenine and formylanthranilate) are also decreased and even those of products in the subsequent reactions, reinforcing the hypothesis that inhibition occurred at the first step. Intriguingly, a similar lower fold change in parasites treated with 10 x EC_{50} was observed for 2-oxoadipate and (S)-3-hydroxybutanoyl-CoA, metabolites much further downstream in this branch of the tryptophan metabolic pathway. The changes in this more distant part of tryptophan catabolism may be either due to CTA having multiple targets along this pathway or allosteric activity regulation by metabolites higher up in the pathway.

The other branch of tryptophan metabolism produces indol-3-pyruvate (I3P) and downstream products such as indol-3-acetaldehyde (I3AA) and indol-3-acetate (I3A) (Figure 2B). Previous studies have demonstrated the excretion of I3P and I3A in high quantity by BSF *T. brucei*, while I3P has been shown to be an important virulence factor (Diskin et al. 2021; EL SAWALHY et al.

1995; Hall, Dahm, et al. 1981; Hall, Dahmt, et al. 1981; McGettrick et al. 2016). In our study, intracellular levels of I3AA were significantly decreased in CTA-treated trypanosomes compared to the controls. Usually, cells catalyze the tryptophan to I3P reaction by an amino oxidase (EC 1.4.1.27) or a devoted tryptophan aminotransferase (EC 2.6.1.27 or EC 2.6.1.99), enzymes which have not (yet) been identified in trypanosomes. Interestingly, Marciano et al. (2008) characterized an aspartate aminotransferase (ASAT; EC 2.6.1.1) that could participate in this pathway. *T. brucei* and *T. cruzi* contain two ASAT isoenzymes; whereas the mitochondrial ASAT is highly specific towards aspartate, its cytosolic counterpart (cASAT) showed broad substrate specificity, with especially the *T. brucei* enzyme having by far the highest affinity and catalytic efficiency (*V*max/*K*m) for tryptophan. It thus seems feasible that the cASAT is a candidate target of CTA.

Inhibition of the cASAT may also affect the levels of other metabolites, like oxaloacetate, which acts as the preferred amino group acceptor in the reaction catalyzed by this enzyme with tryptophan as a donor and leading to the formation of aspartate and I3P (McGettrick et al. 2016), or alternatively 2-oxoglutarate as the acceptor resulting in glutamate production. In order to assess these possible effects, the matched LC-HR-MS database was reviewed in search for these metabolites. A heatmap plotted with additional metabolites, regardless of significance, can be found in Supplementary Data Figure 4. This approach analyzed the data from multiple angles, allowing for pathways and metabolites affected by CTA that might not have been retained by the original mummichog algorithm to be noticed. In this analysis, it became evident that cASAT might indeed be a CTA target due to the lower fold change found for L-aspartate after 10 x EC_{50} treatment. However, the level of the amino group acceptor of cASAT, oxaloacetate, was not found to be increased upon CTA treatment but decreased.

Concerning the ^{1}H-NMR data, 4 out of 59 significant bins were left unidentified since no matches were found to the peaks in the database. The heatmap with the full list and changes according to treatment can be found in Figure 2C. The metabolites associated with each significant bin were explored through pathway analysis of *T. b. brucei* and most pathways found to be significantly altered corresponded to amino acid metabolism. Furthermore, negative fold change for 2-oxoglutarate and the aromatic amino acids tyrosine and phenylalanine for which the cASAT also has appreciable affinity, and positive change for tryptophan upon 10 x EC_{50} CTA treatment further corroborates not only the effects to tryptophan metabolism, but also the possible cASAT

interference (Marciano et al. 2008). Further statistical analysis confirms that 10 x EC_{50} treatment presents more statistically significant differences when compared to the control than to the treatment with 5 x EC_{50} (at FDR threshold of 0.05, Supplementary Data Figure 5). Namely, a higher fold associated with AMP and ADP/ATP when parasites are treated with 10 x EC_{50} when compared to the control, whereas pyruvate and a few amino acids such as glutamate and proline are more present in control samples. Pyruvate levels have been reported to increase in spent medium due to aerobic glycolysis (Creek et al. 2013). Meanwhile, products resulting from deamination of amino acids, *e.g.* tryptophan, tyrosine, phenylalanine, and glutamate have also been reported in the spent medium, and as such, tryptophan increase after CTA treatment supports enzymatic target(s) acting on this amino acid (Creek et al. 2013). Additionally, as mentioned above, since tryptophan fold change increases with CTA treatment, tryptophan transport inhibition doesn't seem to be involved with the compound's mode of action.

Results from both analytical techniques support a CTA target related with tryptophan metabolism, whether on enzymes that directly catalyze reactions involving this amino acid or multiple branched effects.

DISCUSSION

3-*O*-*p*-(*Z/E*)-coumaroyltormentic acids are a mixture of triterpenoid esters with antitrypanosomal activity originally isolated from the leaves of *V. paradoxa*, a plant traditionally used in West Africa for many applications, including food, cosmetic and in traditional medicine (Afolabi et al. 2020). As such, the extraction and isolation of triterpenic esters from another source was important since *V. paradoxa* is considered as vulnerable by the International Union for Conservation of Nature and Natural Resources (Afolabi et al. 2020). 3-*O*-*p*-(*Z/E*)-coumaroyltormentic acids have been reported in other species but in this work, an apple cell culture was used to provide an extract that yielded mostly CTA (Afolabi et al. 2020; Catteau et al. 2021). Other esters were found in this fraction, namely 3-*O*-*p*-(*Z/E*)-feruloyltormentic acids, very close structural compounds also transforming to each other. Little is known about this mixture, except for the reported selective antitrypanosomal activity of the fractions containing CTA (Leclercq et al. 2020; Liao et al. 2019).

Untargeted metabolomics assays performed on *T. b. brucei* exposed for 3 h to CTA as the growth of parasites was severely affected, with dying observed at 5 h when general cellular death pathways are activated. After a 3h treatment with CTA, results revealed effects to tryptophan metabolism.

^{1}H-NMR analysis revealed increased levels of tryptophan when compared to untreated parasites, whereas HR-MS-negative data analysis showed decreased levels of multiple metabolites directly linked to tryptophan. Initial analysis of ^{1}H-NMR data indicated statistically significant differences for multiple amino acids after CTA treatment. However, these differences are likely due to a generalized or indirect effect, seeing that all amino acids are present in the culture medium and that distinct plasma-membrane transporters involved in their uptake have been characterized (Creek et al. 2013; Marchese et al. 2018). Inhibition of the tryptophan transporter is also unlikely because tryptophan's fold change indicates an intracellular accumulation. Despite reports of extraordinary consumption of tryptophan and phenylalanine by *T. b. brucei* in culture, the extracellular presence of only one amino acid, cysteine, was confirmed to be essential for trypanosome growth (Creek et al. 2013). Interestingly, slender BSF trypomastigotes of *T. b. brucei* depend exclusively on glucose for energy, contrarily to the parasite infecting the invertebrate vector, where amino acids, especially proline, are used as fuel through the Krebs cycle (Nowicki and Cazzulo 2008). Thus, our results align with an effect after tryptophan import that might reveal more about this metabolite's role in trypanosome growth (EL SAWALHY et al. 1995; Hall, Dahm, et al. 1981; Hall, Dahmt, et al. 1981).

A potential CTA target in tryptophan metabolism is the KP in which the first reaction is its conversion to N-formyl-kynurenine catalyzed by TDO and/or IDO (Ternes and Schönknecht 2014; Villani et al. 2024). The targeting of any or both of these enzymes would justify the negative fold change after CTA treatment in downstream metabolites found in our study, similar to the tryptophan increase as reported by Villani et al. after ID1 inhibition in melanoma cancer cells (cell line A375). However, each of these two non-homologous enzymes have acquired high sequence variability across eukaryotes and prokaryotes also due to horizontal gene transfers as well as duplications leading to multiple isoforms (Ball et al. 2014). Importantly, TDO/IDO sequences are yet to be identified in *T. b. brucei*. A phylogenetic analysis revealed that the KP too has evolved with numerous gene transfers among species, also in the Excavata, the taxonomic supergroup to which trypanosomes belong (Ternes and Schönknecht 2014). These modifications in different organisms led to changed characteristics and properties, and even functional divergence, notably for IDO homologs, which has generated an enzyme family that has diverged across species. As such, the high variability associated with the genetic sequences for these enzymes might explain the difficulty in finding homologous enzyme(s) in *T. b. brucei*. In attempts to confirm the presence

of a *T. b. brucei* gene encoding IDO or TDO, blastp searches were conducted in the NCBI GenBank (http://blast.ncbi.nlm.nih.gov) by querying the database with different sequences previously identified as IDO or TDO. First, using the *Paratrypanosoma confusum* sequence annotated as TDO in the TriTrypDB (https://tritrypdb.org/tritrypdb/app) (Supplementary Data Table 2). *P. confusum* belongs, like the trypanosomatids, to the Order Kinetoplastea. In agreement with a previous report (Opperdoes et al. 2016), homologs were only found in three other kinetoplastids: *Bodo saltans* and two *Trypanosoma* species (*T. theileri* and *T. melophagium*). These were found to have the highest sequence identity, in addition to many prokaryotes and only a single eukaryote within the top 100 hits, the Excavate protist *Naegleria lovaniensi*. Searches with TDO and IDO sequences from various pro- and eukaryotes did also not identify a homolog in trypanosomatids like *T. brucei*, *T. cruzi* and *Leishmania* species. The finding of a *N. lovaniensi* TDO candidate may indicate that a common ancestor of the Excavata acquired a bacterial TDO gene by horizontal transfer, but the gene may have been replaced again in *T. brucei* and many other trypanosomatids. Alternatively, *T. brucei* might have retained a very different and therefore not yet identified, authentic eukaryotic TDO or IDO gene. Regardless, our current data seems to converge towards the presence of a TDO/IDO and the KP in *T. b. brucei*, which could prove to be a viable pharmacological target in the future.

The effects shown after CTA treatment are not only present in the initial reaction, but also in subsequent reactions catalyzed by kynureninase (EC 3.7.1.3) and kynurenine aminotransferase (also called kynurenine transaminase, KAT, EC 2.6.1.7) (Ecco et al. 2009; Marciano et al. 2009). Kynureninase has been identified in multiple organisms, including in *T. cruzi* in a transcriptomics study, whereas a putative KAT has been described for *T. brucei* (Ecco et al. 2009; Marciano et al. 2009). Interestingly, in this *T. brucei*, the KAT turned out to have higher affinity towards L-cysteine and L-glutamine while being able to use different 2-oxoacids as amino acceptors (Marciano et al. 2008). It could be that it regulates levels of 2-oxoacids and maintains amino acids balance as do mammalian KATs. Conversely, it is possible that the *Trypanosoma* cASAT, with its broad substrate specificity, is also responsible for the KAT activity, similar as reported for the *Escherichia coli* and mouse mitochondrial ASATs (Q. Han et al. 2001; Qian Han et al. 2011). An enzyme with such multiple activities would justify, after inhibition, a profile in which multiple amino acids and metabolites of tryptophan metabolism are affected, as seen in our study. Furthermore, studies on cASAT of *T. brucei* have demonstrated a higher substrate affinity to

tryptophan than for aspartate itself, supporting the hypothesis that a demonstrated inhibition on these enzymes would relate to tryptophan (Marciano et al. 2008).

Whereas the intracellular level of tryptophan, the amino group donor of cASAT, was increased after CTA treatment, that of its preferred amino group acceptor, oxaloacetate, was unexpectedly found to be decreased. This may have been due to a considerable decrease in its formation, that in BSF *T. brucei* occurs mainly by phosphoenolpyruvate carboxykinase in the succinate-producing branch of glycolysis (reviewed in (Michels et al. 2021)). Indeed, also levels of the other intermediates of this branch dropped after CTA treatment: phosphoenolpyruvate, malate, fumarate and succinate (Supplementary Data Figure 4). It is conceivable that this is caused by a decrease in glucose metabolism, or that a major part of the glucose 6-phosphate is redirected from the glycolytic pathway to the pentose-phosphate pathway in an attempt by the cell to deal with the stress resulting from the toxic effects of CTA.

Despite the identification of KP intermediates in *T. brucei* and the presence of various (candidate) enzymes involved in the TriTrypDB, the precise role of the pathway in the parasite's biology remains to be established. In many organisms, KP is important for NAD^+ biosynthesis (Ternes and Schönknecht 2014), however not in trypanosomes that rely on purine salvage (reviewed in (Hofer 2023)). The complete KP as depicted in KEGG has many branches enabling the formation of a large variety of metabolites, at least some of them potentially also important in these parasites.

Trypanosomatids are auxotroph for aromatic amino acids and depend on their uptake from the environment (Marchese et al. 2018). Our analysis strongly suggests that in *T. b. brucei*, cASAT catalyzes a reaction from tryptophan that leads to I3P, that can subsequently be converted in other indole metabolites, namely I3AA, indole-3-lactate, I3A and indole-3-ethanol. These metabolites have not been reported for all trypanosomatids, but animals infected with *T. b. gambiense* and *T. b. evansi* have increased levels of them in urine and blood (EL SAWALHY et al. 1995; Hall, Dahm, et al. 1981; Hall, Dahmt, et al. 1981; McGettrick et al. 2016). These end products are thought to be rapidly excreted into the medium by *in vitro* grown *T. b. evansi*, so analysis of the culture media in this study would have been important to confirming the effects on this branch of tryptophan metabolism (EL SAWALHY et al. 1995; McGettrick et al. 2016). Additionally, I3P is reportedly chemically unstable, which could justify why it was not detected in our study. Still, the effects found here to I3AA and I3A support an effect on this pathway, with potential inhibition of cASAT

(Nowicki and Cazzulo 2008). This is further confirmed by the negative fold change found for L-aspartate after CTA treatment. cASAT has been shown to be essential for growth of BSF trypanosomes in an RNA interference (RNAi) experiment (McGettrick et al. 2016). This deleterious effect on growth was attributed to the decreased intracellular level of aspartate. This metabolite is essential in purine salvage and *de novo* pyrimidine biosynthesis but has a low uptake rate in *T. brucei*. The fact that RNAi for cASAT eliminated most of the I3P excretion renders it unlikely that other enzymes acting on aromatic amino acids, such as tyrosine aminotransferase (TAT), play a major role in it. As such, it is plausible that the parasite's main source of L-aspartate is the cASAT catalyzed reactions. *T. brucei* cASAT reportedly has a greater preference for tryptophan as the amino group donor, which is in line with a preferential target by CTA in our study (McGettrick et al. 2016). Furthermore, in *T. cruzi*, enzymes related to the catabolism of aromatic amino acids have been correlated to cytosolic NADH synthesis, furthering the potential essentiality of this pathway (Nowicki and Cazzulo 2008).

It is impossible to exclude the possibility of multiple targets or upstream regulation as cascade effects of CTA. Negative fold change of 2-oxoadipate and (S)-3-hydroxy butanoyl-CoA could be indicative of acetyl-CoA changes and, as such, energetic and fatty acid/lipid changes. However, due to the availability of glucose and lipids in the medium, and in the mammalian's host serum, effects to these pathways are likely not the main mode of action of CTA, as it would not justify its good antitrypanosomal activity. Multiple additional changes to the parasite's metabolome were detected. These could be indicative of secondary effects occurring after the 3 h treatment. Proteolysis could be involved, justifying a higher detection of amino acids by NMR.

Despite the current lack of data about the presence of tryptophan degradation pathways in trypanosomatids, our results support the presence of this part of amino acid metabolism and, moreover, demonstrate its targetability for drugs. The broad enzymatic specificity of *T. brucei* cASAT is not only important in the context of the parasite's amino acid metabolism, but due to its demonstrated high tryptophan affinity, potential KAT activity and continuous expression in BSF, also important in the context of CTA's antitrypanosomal activity (Marciano et al. 2008, 2009). However, it remains necessary to ascertain the presence of enzymes catalyzing tryptophan degradation, maybe after using more bespoke bioinformatic approaches, and to confirm experimentally their substrate specify and essentiality to the trypanosome. Finally, trypanosome

tryptophan metabolism could be linked with the pathogenesis of trypanosomiasis not only in animals, but also in humans by interfering with serotonin levels, while there are studies reporting important virulence roles of excreted indole-3-pyruvate, which as mentioned previously, is an important tryptophan degradation metabolite (Ball et al. 2014; Diskin et al. 2021; McGettrick et al. 2016; Nowicki and Cazzulo 2008). Our results strongly suggest that our natural compound CTA exerts antitrypanosomal activity by interfering with tryptophan metabolism, which would justify the *in vivo* results previously reported, and should support further the interest in studying and uncovering potentially antitrypanosomal targets in this pathway. In the future, CTA's activity should be confirmed by measuring its effect directly on cASAT activity, either in *T. brucei* lysates or using the purified recombinant enzyme, or by using ^{13}C or ^{15}N-labeled tryptophan to detect this important amino acid and downstream metabolites. Since a cASAT RNAi cell line is available, the effect of CTA on this cell line could be investigated to confirm if cASAT is the actual target of CAT.

CONCLUSION

This untargeted metabolomics study of the effects of CTA on BSF *T. b. brucei* revealed notable changes to multiple metabolites in the tryptophan degradation pathway. Despite the fact that the existence of enzymes catalyzing the initial conversion of tryptophan in trypanosomes remains to be proved, our metabolomics data offer solid indirect evidence of the presence of these enzymes, notably TDO/IDO, ASAT and KAT. The current absence of some of them in the database, or for others the annotation as 'hypothetical' because of an unusual sequence or possession of unusually broad substrate specificity of a known enzyme could explain why some of these enzymes have not yet been described for *T. brucei.* Our results indicate that amino acid degradation pathways could constitute potential antitrypanosomal targets and incentivize their experimental characterization in future studies.

Figures list:

Figure 1. 1) PCA scores plot and 2) PLS-DA projections of treatment groups according to the first two principal components for MS-negative (A), MS-positive (B) and ^{1}H-NMR (C) analyses. Red nodes correspond to samples of the control group, green and blue nodes correspond to 5 x and 10 x EC_{50}, respectively.

Figure 2. A) Heatmap of the statistically significantly impacted metabolites of tryptophan metabolism (Table 1) (after Pareto scaling of LC-MS data). B) Schematic view of the potential tryptophan metabolism in the trypomastigote's cytosol. ADP – adenosine diphosphate, ASAT – aspartate aminotransferase, ATP – adenosine triphosphate, CTA – 3-O-*p*-(*Z*/*E*)-coumaroyltormentic acids, I3A – indol-3-acetate, I3P – indol-3-pyruvate, I3AA – indol-3-acetaldehyde, IDO – indoleamine 2,3-dioxygenase, KAT – kynurenine transaminase, PEP – phosphoenolpyruvate, TAT – tyrosine aminotransferase, TDO – tryptophan 2,3-dioxygenase. Red bold – enzymes, arrow in orange – positive fold change, arrow in blue – negative fold change. Created in BioRender.com. C) Heatmap of the ANOVA bins of ^{1}H-NMR data – lines correspond to the annotated bins.

ACKNOWLEDGMENTS

The authors would like to thank Sylvain Legay for *in vitro*-cultivated apple cells. This work was supported by the Belgian National Fund for Scientific Research (FNRS, grant PDR T.0092.20).

REFERENCES

Adusumilli, R., & Mallick, P. (2017). Data Conversion with ProteoWizard msConvert. *Methods in Molecular Biology (Clifton, N.J.)*, *1550*, 339–368. https://doi.org/10.1007/978-1-4939-6747-6_23

Afolabi, J. O., Olorode, E. M., Olomola, D. B., Fasakin, Y. O., & Adekunle, E. A. (2020). Effects of different media strengths and hormone concentrations on in-vitro regeneration of *Vitellaria paradoxa* C.F. Gaertn. *Nigerian Journal of Biotechnology*, *37*(1), 150–158. https://doi.org/10.4314/njb.v37i1.16

Ball, H. J., Jusof, F. F., Bakmiwewa, S. M., Hunt, N. H., & Yuasa, H. J. (2014). Tryptophan-catabolizing enzymes - party of three. *Frontiers in Immunology*, *5*(OCT), 1–10. https://doi.org/10.3389/fimmu.2014.00485

Barrett, M. P., Priotto, G., Franco, J. R., Lejon, V., & Lindner, A. K. (2024). Elimination of human African trypanosomiasis: The long last mile. *PLOS Neglected Tropical Diseases*, *18*(5), e0012091. https://doi.org/10.1371/journal.pntd.0012091

Biebinger, S., Elizabeth Wirtz, L., Lorenz, P., & Christine Clayton. (1997). Vectors for inducible expression of toxic gene products in bloodstream and procyclic Trypanosoma brucei. *Molecular and Biochemical Parasitology*, *85*(1), 99–112. https://doi.org/10.1016/S0166-6851(96)02815-0

Catteau, L., Schioppa, L., Beaufay, C., Girardi, C., Hérent, M.-F., Frédérich, M., & Quetin-Leclercq, J. (2021). Antiprotozoal activities of Triterpenic Acids and Ester Derivatives Isolated from the Leaves of Vitellaria paradoxa. *Planta Medica*, *87*(10–11), 860–867. https://doi.org/10.1055/a-1286-1879

Chong, J., Wishart, D. S., & Xia, J. (2019). Using MetaboAnalyst 4.0 for Comprehensive and Integrative Metabolomics Data Analysis. *Current Protocols in Bioinformatics*, *68*(1), 1–128. https://doi.org/10.1002/cpbi.86

Creek, D. J., Nijagal, B., Kim, D.-H., Rojas, F., Matthews, K. R., & Barrett, M. P. (2013). Metabolomics Guides Rational Development of a Simplified Cell Culture Medium for Drug Screening against Trypanosoma brucei. *Antimicrobial Agents and Chemotherapy*, *57*(6), 2768–2779. https://doi.org/10.1128/AAC.00044-13

Diskin, C., Corcoran, S. E., Tyrrell, V. J., McGettrick, A. F., Zaslona, Z., O'Donnell, V. B., et al. (2021). The Trypanosome-Derived Metabolite Indole-3-Pyruvate Inhibits Prostaglandin Production in Macrophages by Targeting COX2. *The Journal of Immunology*, *207*(10), 2551–2560. https://doi.org/10.4049/jimmunol.2100402

562 Ecco, G., Vernal, J., Razzera, G., Tavares, C., Serpa, V. I., Arias, S., et al. (2009). Initial
563 characterization of a recombinant kynureninase from Trypanosoma cruzi identified from
564 an EST database. *Gene*, *448*(1), 1–6. https://doi.org/10.1016/j.gene.2009.08.007
565 EL SAWALHY, A., SEED, J. R., EL ATTAR, H., & HALL, J. E. (1995). Catabolism of
566 Tryptophan by Trypanosoma evansi. *Journal of Eukaryotic Microbiology*, *42*(6), 684–690.
567 https://doi.org/10.1111/j.1550-7408.1995.tb01616.x
568 Fall, F., Desmet, L., Mamede, L., Schioppa, L., De Tullio, P., Frédérich, M., et al. (2024).
569 Comparison of Three Widely Employed Extraction Methods for Metabolomic Analysis of
570 *Trypanosoma brucei*. *Current Protocols*, *4*(5), e1043. https://doi.org/10.1002/cpz1.1043
571 Fall, F., Mamede, L., Schioppa, L., Ledoux, A., De Tullio, P., Michels, P., et al. (2022).
572 Trypanosoma brucei: Metabolomics for analysis of cellular metabolism and drug discovery.
573 *Metabolomics*, *18*(4), 20. https://doi.org/10.1007/s11306-022-01880-0
574 Féraud, B., Munaut, C., Martin, M., Verleysen, M., & Govaerts, B. (2017). Combining strong
575 sparsity and competitive predictive power with the L-sOPLS approach for biomarker
576 discovery in metabolomics. *Metabolomics*, *13*(11), 1–15. https://doi.org/10.1007/s11306-
577 017-1275-y
578 Franco, J., Scarone, L., & Comini, M. A. (2018). Chapter Three - Drugs and Drug Resistance in
579 African and American Trypanosomiasis. In M. Botta (Ed.), *Annual Reports in Medicinal*
580 *Chemistry* (Vol. 51, pp. 97–133). Academic Press.
581 https://doi.org/10.1016/bs.armc.2018.08.003
582 Giacomoni, F., Le Corguillé, G., Monsoor, M., Landi, M., Pericard, P., Pétéra, M., et al. (2015).
583 Workflow4Metabolomics: a collaborative research infrastructure for computational
584 metabolomics. *Bioinformatics*, *31*(9), 1493–1495.
585 https://doi.org/10.1093/bioinformatics/btu813

Hall, J. E., Dahm, K. H., & Seed, J. R. (1981). Quantification of tryptophan catabolites from Trypanosoma brucei gambiense in vitro. *Comp. Biochem. Physiol., 68B*, 521–526. https://doi.org/0305-0491/81/040521-06802.00/0

Hall, J. E., Dahmt, K. H., & Seed, J. R. (1981). In vitro tryptophan catabolism by Trypanosoma (Trypanozoon) brucei gambiense, T. (T.) equiperdum, T. (herpetosoma) lewisi and T. (h.) musculi. *Comp., 69B*, 617–620. https://doi.org/0305-0491/81/070617-04802.00/0

Han, Q., Fang, J., & Li, J. (2001). Kynurenine aminotransferase and glutamine transaminase K of Escherichia coli: Identity with aspartate aminotransferase. *Biochemical Journal*, *360*(3), 617–623. https://doi.org/10.1042/0264-6021:3600617

Han, Qian, Robinson, H., Cai, T., Tagle, D. A., & Li, J. (2011). Biochemical and structural characterization of mouse mitochondrial aspartate aminotransferase, a newly identified kynurenine aminotransferase-IV. *Bioscience Reports*, *31*(5), 323–332. https://doi.org/10.1042/BSR20100117

Hannaert, V. (2011). Sleeping sickness pathogen (Trypanosoma brucei) and natural products: therapeutic targets and screening systems. *Planta Medica*, *77*(6), 586–597. https://doi.org/10.1055/s-0030-1250411

Hirumi, H., & Hirumi, K. (1994). Axenic culture of African trypanosome bloodstream forms. *Parasitology Today*, *10*(2), 80–84. https://doi.org/10.1016/0169-4758(94)90402-2

Hofer, A. (2023). Targeting the nucleotide metabolism of *Trypanosoma brucei* and other trypanosomatids. *FEMS Microbiology Reviews*, *47*(3), fuad020. https://doi.org/10.1093/femsre/fuad020

Johnston, K., Kim, D.-H., Kerkhoven, E. J., Burchmore, R., Barrett, M. P., & Achcar, F. (2019). Mapping the metabolism of five amino acids in bloodstream form *Trypanosoma brucei*

using U-13C-labelled substrates and LC–MS. *Bioscience Reports*, *39*(5), BSR20181601. https://doi.org/10.1042/BSR20181601

Karaman, İ., Nørskov, N. P., Yde, C. C., Hedemann, M. S., Bach Knudsen, K. E., & Kohler, A. (2015). Sparse multi-block PLSR for biomarker discovery when integrating data from LC–MS and NMR metabolomics. *Metabolomics*, *11*(2), 367–379. https://doi.org/10.1007/s11306-014-0698-y

Kasozi, K. I., MacLeod, E. T., Ntulume, I., & Welburn, S. C. (2022). An Update on African Trypanocide Pharmaceutics and Resistance. *Frontiers in Veterinary Science*, *9*(March). https://doi.org/10.3389/fvets.2022.828111

Leclercq, J., Beaufay, C., Catteau, L., Andre, C., & Legay, S. (2020, August 13). METHOD FOR PRODUCING A COMPOSITION COMPRISING A 3-O-p-COUMAROYL ESTER OF TORMENTIC ACID FROM A PLANT CELL CULTURE, APPLICATIONS THEREOF AS ANTIPARASITIC AGENT FOR THE TREATMENT OF TRYPANOSOMIASIS. https://patents.google.com/patent/WO2020161221A1/en. Accessed 2 October 2023

Li, S., Park, Y., Duraisingham, S., Strobel, F. H., Khan, N., Soltow, Q. A., et al. (2013). Predicting Network Activity from High Throughput Metabolomics. *PLOS Computational Biology*, *9*(7), e1003123. https://doi.org/10.1371/journal.pcbi.1003123

Liao, X., Hu, F., & Chen, Z. (2019). A HPLC-MS method for profiling triterpenoid acids and triterpenoid esters in *Osmanthus fragrans* fruits. *The Analyst*, *144*(23), 6981–6988. https://doi.org/10.1039/C9AN01542F

Marchese, L., Nascimento, J. D. F., Damasceno, F. S., Bringaud, F., Michels, P. A. M., & Silber, A. M. (2018). The uptake and metabolism of amino acids, and their unique role in the biology of pathogenic trypanosomatids. *Pathogens*, *7*(2), 1–45. https://doi.org/10.3390/pathogens7020036

Marciano, D., Llorente, C., Maugeri, D. A., de la Fuente, C., Opperdoes, F., Cazzulo, J. J., & Nowicki, C. (2008). Biochemical characterization of stage-specific isoforms of aspartate aminotransferases from Trypanosoma cruzi and Trypanosoma brucei. *Molecular and Biochemical Parasitology*, *161*(1), 12–20. https://doi.org/10.1016/j.molbiopara.2008.05.005

Marciano, D., Maugeri, D. A., Cazzulo, J. J., & Nowicki, C. (2009). Functional characterization of stage-specific aminotransferases from trypanosomatids. *Molecular and Biochemical Parasitology*, *166*(2), 172–182. https://doi.org/10.1016/j.molbiopara.2009.04.001

McGettrick, A. F., Corcoran, S. E., Barry, P. J. G., McFarland, J., Crès, C., Curtis, A. M., et al. (2016). Trypanosoma brucei metabolite indolepyruvate decreases HIF-1α and glycolysis in macrophages as a mechanism of innate immune evasion. *Proceedings of the National Academy of Sciences of the United States of America*, *113*(48), E7778–E7787. https://doi.org/10.1073/pnas.1608221113

Michels, P. A. M., Villafraz, O., Pineda, E., Alencar, M. B., Cáceres, A. J., Silber, A. M., & Bringaud, F. (2021). Carbohydrate metabolism in trypanosomatids: New insights revealing novel complexity, diversity and species-unique features. *Experimental Parasitology*, *224*, 108102. https://doi.org/10.1016/j.exppara.2021.108102

Nowicki, C., & Cazzulo, J. J. (2008). Aromatic amino acid catabolism in trypanosomatids. *Comparative Biochemistry and Physiology - A Molecular and Integrative Physiology*, *151*(3), 381–390. https://doi.org/10.1016/j.cbpa.2007.03.010

Opperdoes, F. R., Butenko, A., Flegontov, P., Yurchenko, V., & Lukeš, J. (2016). Comparative Metabolism of Free-living Bodo saltans and Parasitic Trypanosomatids. *The Journal of eukaryotic microbiology*, *63*(5), 657–678. https://doi.org/10.1111/jeu.12315

Pink, R., Hudson, A., Mouriès, M.-A., & Bendig, M. (2005). Opportunities and challenges in antiparasitic drug discovery. *Nature Reviews. Drug Discovery*, *4*(9), 727–740. https://doi.org/10.1038/nrd1824

Sumner, L. W., Amberg, A., Barrett, D., Beale, M. H., Beger, R., Daykin, C. A., et al. (2007). Proposed minimum reporting standards for chemical analysis: Chemical Analysis Working Group (CAWG) Metabolomics Standards Initiative (MSI). *Metabolomics*, *3*(3), 211–221. https://doi.org/10.1007/s11306-007-0082-2

Ternes, C. M., & Schönknecht, G. (2014). Gene transfers shaped the evolution of de novo NAD+ biosynthesis in eukaryotes. *Genome Biology and Evolution*, *6*(9), 2335–2349. https://doi.org/10.1093/gbe/evu185

Villani, S., Fallarini, S., Rezzi, S. J., Di Martino, R. M. C., Aprile, S., & Del Grosso, E. (2024). Selective inhibition of indoleamine and tryptophan 2,3-dioxygenases: Comparative study on kynurenine pathway in cell lines via LC-MS/MS-based targeted metabolomics. *Journal of Pharmaceutical and Biomedical Analysis*, *237*(June 2023), 115750. https://doi.org/10.1016/j.jpba.2023.115750

WHO | Human African trypanosomiasis. (n.d.). *WHO*. World Health Organization. http://www.who.int/trypanosomiasis_african/en/. Accessed 30 June 2020

Wiedemar, N., Hauser, D. A., & Mäser, P. (2020). 100 Years of Suramin. *Antimicrobial Agents and Chemotherapy*, *64*(3). https://doi.org/10.1128/AAC.01168-19

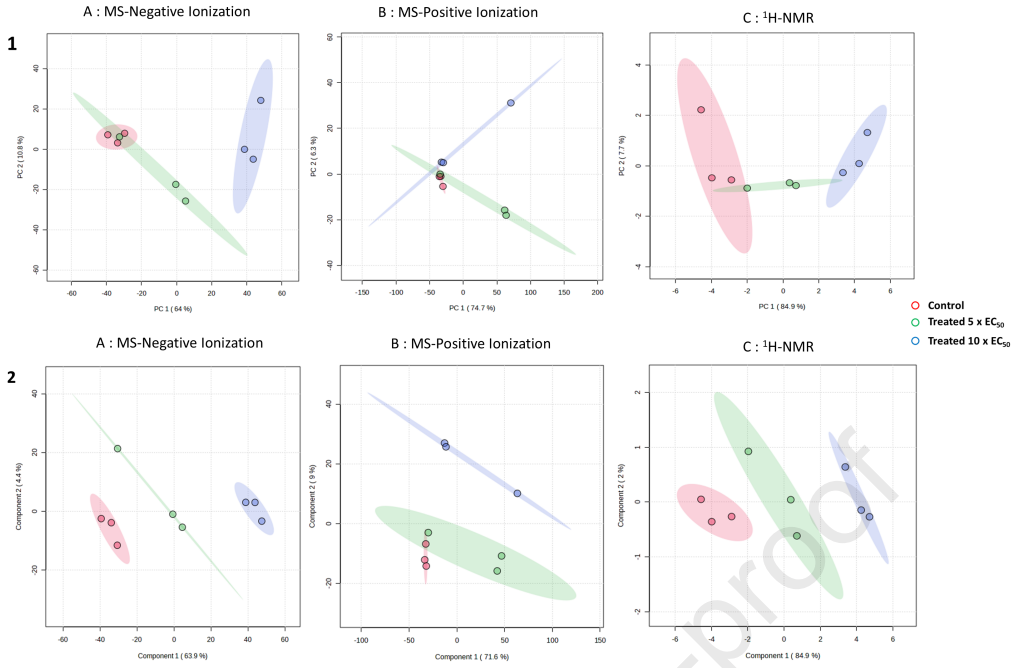

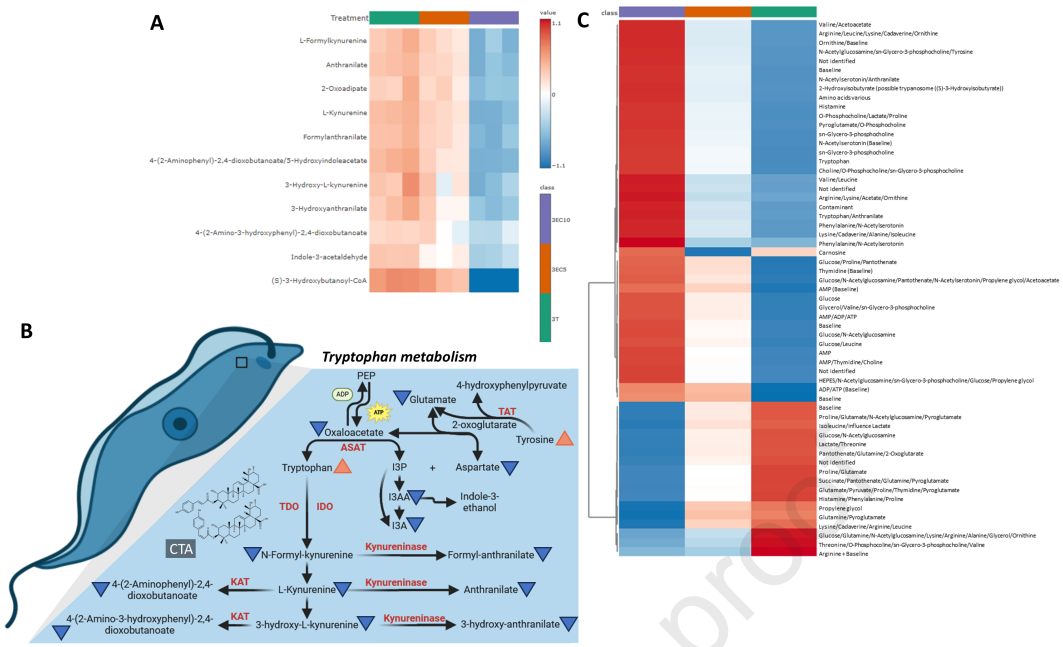

The authors declare that they have no known competing financial interests or personal relationships that could have appeared to influence the work reported in this article.